Supplementary Material (ESI) for Chemical Communications

Electronic Supplementary Information

A novel type of heteropolyoxoanion precursors $\{[Ca(H_2O)]_6[P_4M_6O_{34}]_2\}^{12-}$ ($M = W^{VI}$, Mo^{VI}) constructed by two unique $[P_4M_6O_{34}]^{12-}$ subunits via a rare hexa-calcium cluster

Jingping Wang, Junwei Zhao, Pengtao Ma, Junchuang Ma, Linping Yang, Yan Bai, Mingxue Li, and Jingyang Niu*

Institute of Molecular and Crystal Engineering, College of Chemistry and Chemical Engineering, Henan University
Kaifeng, Henan 475004, China

1. The influences of the pH value on the stability of **1** and **2** in the aqueous solution.
2. Electrochemical properties of **1** and **2** in 0.5 M Na_2SO_4 aqueous solution as the supporting electrolyte.

1. The influences of the pH value on the stability of 1 and 2 in the aqueous solution.

As shown in Fig. S5a, when the acidity of solution of **1** gradually becomes stronger, the absorption band at ca. 210 nm wanes until disappears meanwhile a new absorption band at ca. 250 nm begins to appear, which shows that the $\{[Ca(H_2O)]_6[P_4W_6O_{34}]_2\}^{12-}$ HPOA may be slowly transformed into the predominantly Keggin-type species upon addition of diluted HCl solution. Such presupposition is supported by comparisons of UV spectra between the acidic solution (pH < 4) of $\{[Ca(H_2O)]_6[P_4W_6O_{34}]_2\}^{12-}$ and the acidic solution of Keggin-type species (Fig. S8). As shown in Fig. S8, the newly discoverable band at ca. 250 nm is attributed to the dπ-pπ charge transitions of $O_{b,c} \rightarrow W$ bond of Keggin species, which is the characteristic absorption band of Keggin-type HPOA.[1] However, when the acidity of solution of **2** becomes stronger, the $\{[Ca(H_2O)]_6[P_4Mo_6O_{34}]_2\}^{12-}$ HPOA is not transformed into the Keggin-type HPOA but a Strandberg-type $[P_2Mo_5O_{23}]^{6-}$ HPOA (Fig. S9), fortunately, this Strandberg-type $[P_2Mo_5O_{23}]^{6-}$ HPOA has been successfully isolated by us and structurally determined by single-crystal X-ray diffraction (Fig. S10).[2] On contrast, when the alkalinity of solution of **1** becomes stronger (Fig. S5b), the absorption band at ca. 210 nm also is more and more weak until withers away whereas the solution absorbance becomes larger, indicating that the $\{[Ca(H_2O)]_6[P_4W_6O_{34}]_2\}^{12-}$ HPOA may be gradually decomposed to WO_4^{2-} and PO_4^{3-} ions, which are also explained by the UV spectra of the mixture of $Na_2WO_4{\cdot}2H_2O$ and Na_2HPO_4 with the molar ratio of 3:2 (Fig. S11). But this situation for **2** is also different, when the acidity of solution of **2** becomes stronger, the $\{[Ca(H_2O)]_6[P_4Mo_6O_{34}]_2\}^{12-}$ HPOA is not transformed into unidentified species (Fig. S12).

1 (a) H. So and M. T. Pope, *Inorg. Chem.*, 1972, **7**, 1441; (b) M. T. Pope, *Heteropoly and Isopoly Oxometalates*, Springer, Berlin, 1983; (c) E. B. Wang, C. W. Hu and L. Xu, *Introduction of Polyacid Chemistry*, Chemical Industry Press, Beijing, 1998.

2 $K_3CaH[P_2Mo_5O_{23}]{\cdot}10H_2O$: monoclinic, $P2_1/c$, a = 10.392(4), b = 18.931(7), c = 16.180(6) Å, β = 105.632(5)º, V = 3065.4(18) Å^3, Z = 4, $GOOF$ = 1.004, R_1 = 0.0217, wR_2 = 0.0634.

2. Electrochemical properties of 1 and 2 in 0.5 M Na_2SO_4 aqueous solution as the supporting electrolyte.

In order to explore the electrochemical behaviors of **1** and **2**, we carried out cyclic voltammetric measurements. Fig. S19 and S20 show the evolution of the corresponding cyclic voltammogram for 1 mM **1** (at this point, pH = 6.46) and 1 mM **2** (at this point, pH = 6.49) in the presence of 0.5 M Na_2SO_4 as the supporting electrolyte, respectively. The cyclic voltammogram of **1** (Fig. S19) displays five oxidation peaks (oxidation potentials: –1.177, –1.011, –0.836, –0.475 and 0.024 V) and four reduction peaks (reduction potentials: –1.311, –1.087, –0.907 and –0.589 V). Obviously, the oxidation peak at 0.024 V does not have the corresponding reduction peak. The peak potential separations of the other four pairs of redox peaks are 134, 76, 71 and 114 mV, which are involved in one-electron transfer processes. However, the cyclic voltammogram of **2** (Fig. S20) displays two oxidation peaks (oxidation potentials: –0.774 and 0.020 V) and two reduction peaks (reduction potentials: –1.097 and –0.547 V). The peak potential separations of two pairs of redox peaks are 323 and 567 mV, indicating that both redox processes are irreversible. Furthermore, the cyclic voltammetric measurements of **1** and **2** at different pH values were performed in 0.5 M Na_2SO_4 aqueous solution as the supporting electrolyte (Fig. S13-16). For **1**, when the pH values vary in the range of 4.55–9.45, the peak shapes, numbers and positions of the redox waves hardly change much, suggesting that the $\{[Ca(H_2O)]_6[P_4W_6O_{34}]_2\}^{12-}$ HPOA is still retained between 4.55 and 9.45, which is in good agreement with the results of UV spectra (Fig. S13-14). At pH lower than 4.55 or pH higher than 9.45, the peak shapes, peak numbers, peak positions and peak intensities also change, indicating that the structure of **1** has transformed or decomposed, which is also consonant with the results of UV spectra. Similarly, for **2**, the cyclic voltammograms at different pH values exhibit that the $\{[Ca(H_2O)]_6[P_4Mo_6O_{34}]_2\}^{12-}$ HPOA are stable between 4.85 and 9.00 (Fig. S15-16), which is approximately consistence with the results of UV spectra. In addition, the effect of scan rates on the electrochemical behaviors of **1** and **2** were investigated in the above-mentioned condition, and the plots of peak currents versus scan rates are shown in Fig. S19 and Fig. S20. When the scan rates vary from 20 to 230 mV s^{-1}, the peak currents are proportional to the scan rates, suggesting that the redox processes of **1** and **2** are surface-confined.

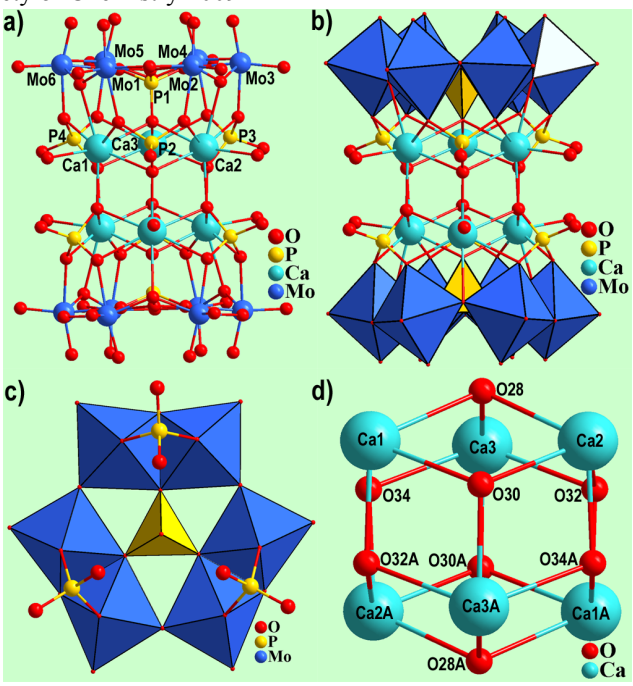

Fig. S1. (a) Ball-and-stick representation of **2** with selected labelling scheme. (b) Combined polyhedral / ball-and-stick representation of **2**. (c) The unique $[P_4Mo_6O_{34}]^{12-}$ subunit with selected labelling scheme in **2**. (d) The hexa-calcium octahedral cluster sandwiched by two unique $[P_4Mo_6O_{34}]^{12-}$ subunits. Atoms with "A" in their labels are symmetrically generated (A: 1 – *x*, –*y*, 2 – *z*).

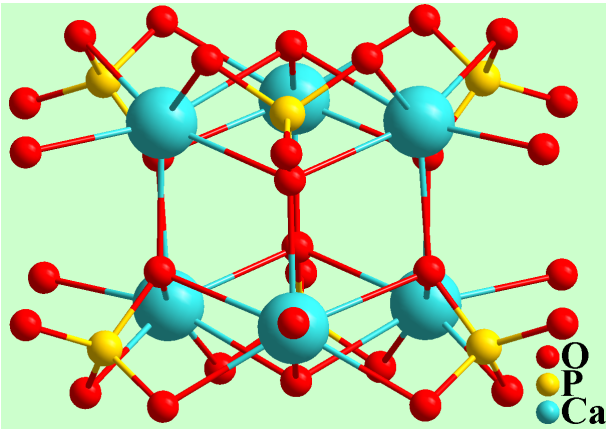

Fig. S2. The resulting calcium phosphate cluster $\{Ca_6(H_2O)_6P_6O_{26}\}$.

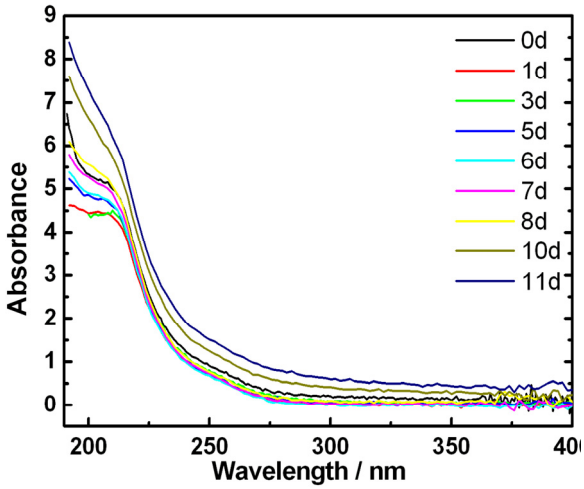

Fig. S3. The influence of time on the stability of **1a** in the aqueous solution. Conditions: the pH value that **1a** was dissolved in water (5×10^{-5} mol L^{-1}) is 6.46.

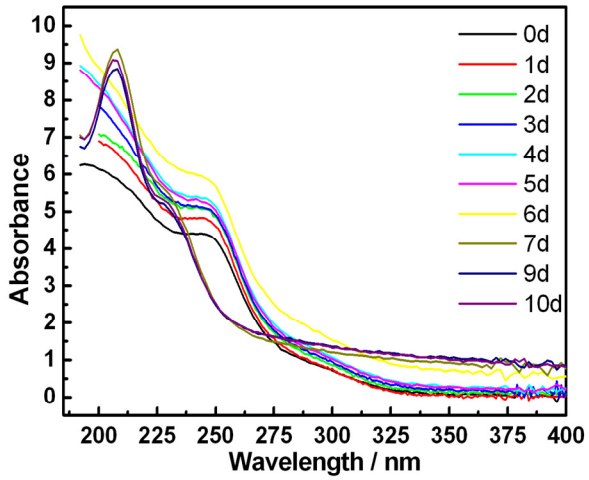

Fig. S4. The influence of time on the stability of **2a** in the aqueous solution. Conditions: the pH value that **2a** was dissolved in water (5×10^{-5} mol L^{-1}) is 6.50.

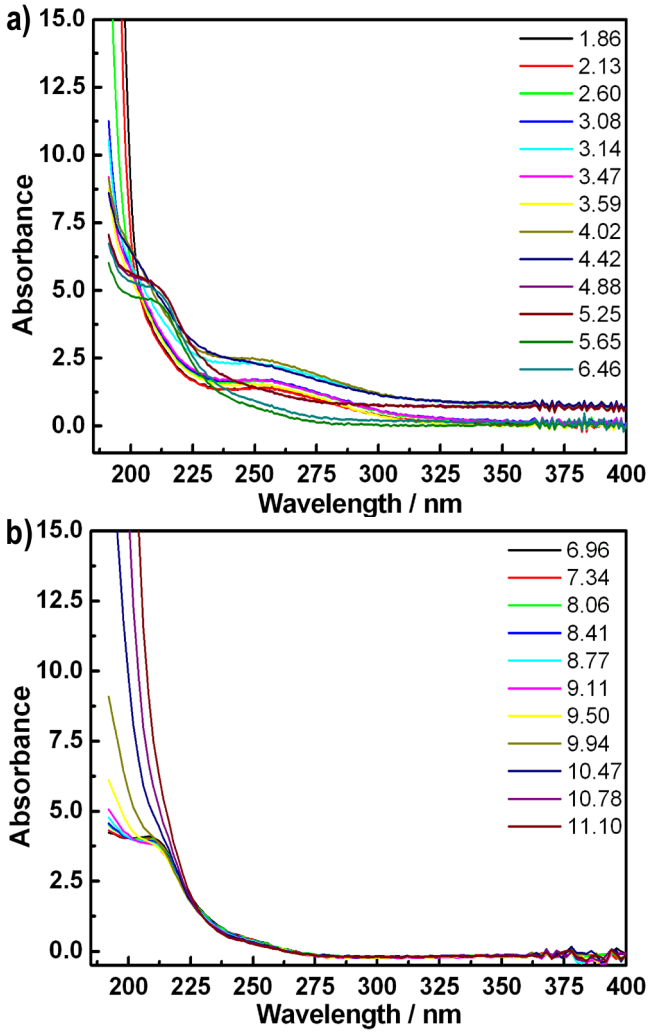

Fig. S5. The influence of the pH value on the stability of **1a** in the aqueous solution: (a) The UV spectral evolution in the acidic direction; (b) The UV spectral evolution in the alkaline direction. Conditions: the pH value that **1a** was dissolved in water (5×10^{-5} mol L^{-1}) is 6.46; the pH values of the acidic direction were adjusted using diluted HCl solution while the pH values of the alkaline direction were adjusted using diluted NaOH solution.

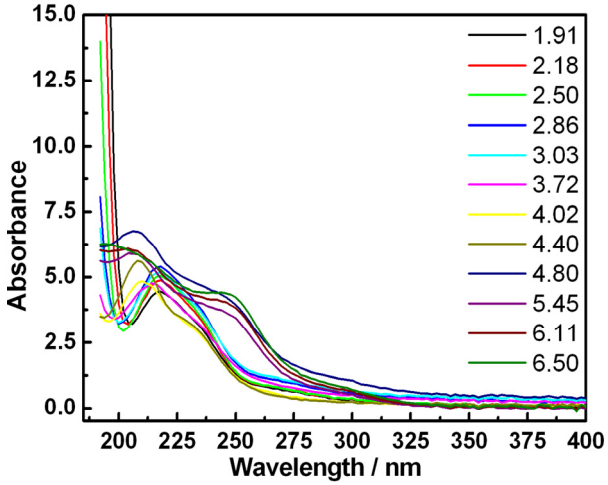

Fig. S6. The UV spectral evolution in the acidic direction. Conditions: the pH value that **2a** was dissolved in water (5×10^{-5} mol L^{-1}) is 6.50; the pH values of the acidic direction were adjusted using diluted HCl solution.

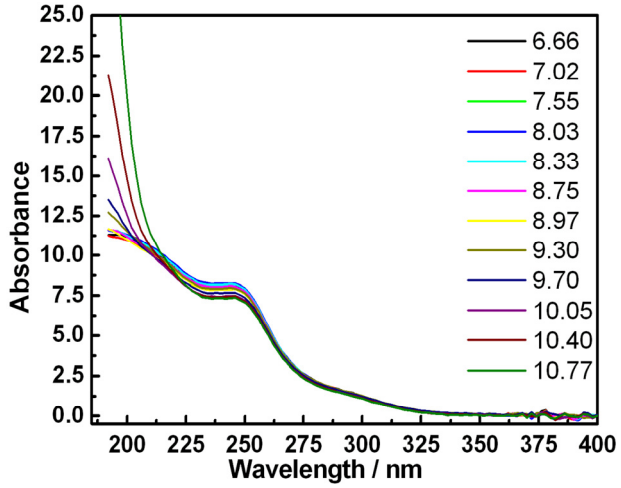

Fig. S7. The UV spectral evolution in the alkaline direction. Conditions: the pH value that **2a** was dissolved in water (5×10^{-5} mol L^{-1}) is 6.50; the pH values of the alkaline direction were adjusted using diluted NaOH solution.

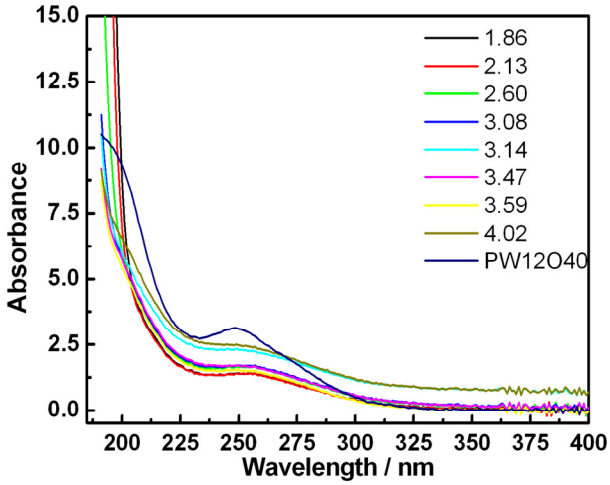

Fig. S8. Comparison between the UV spectra of **1** (pH < 4.40) and the UV spectrum of $[PW_{12}O_{40}]^{3-}$.

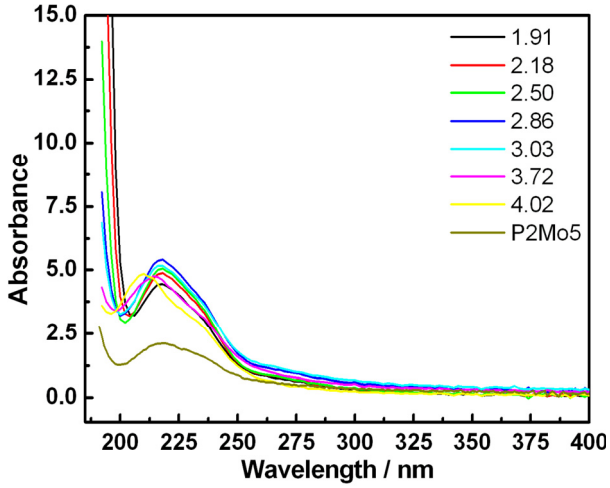

Fig. S9. Comparison between the UV spectra of **2** (pH < 4.40) and the UV spectrum of $[P_2Mo_5O_{23}]^{6-}$.

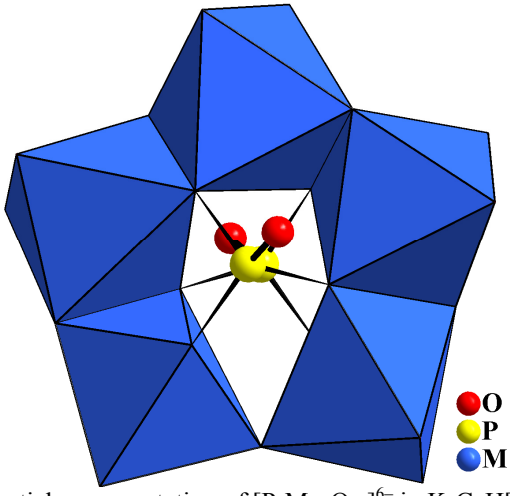

Fig. S10. Combined polyhedral/ball-and-stick representation of $[P_2Mo_5O_{23}]^{6-}$ in $K_3CaH[P_2Mo_5O_{23}]\cdot 10H_2O$.

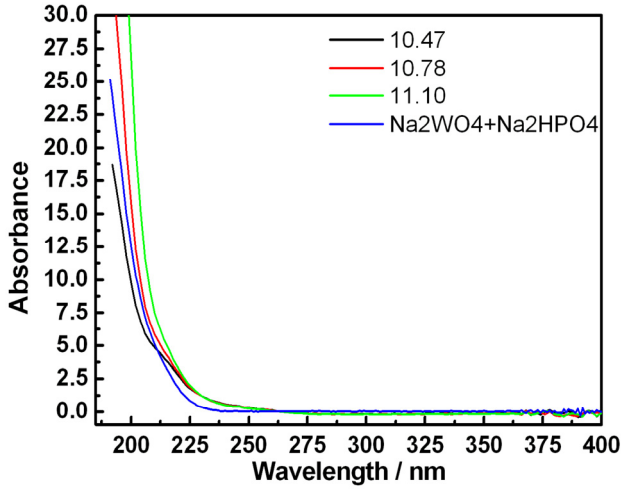

Fig. S11. Comparison between the UV spectra of **1** (pH > 9.94) and the UV spectrum of the mixture of $Na_2WO_4\cdot 2H_2O$ and Na_2HPO_4 with the molar ratio of 3:2 (pH = 10.50). The pH values were adjusted using diluted NaOH solution.

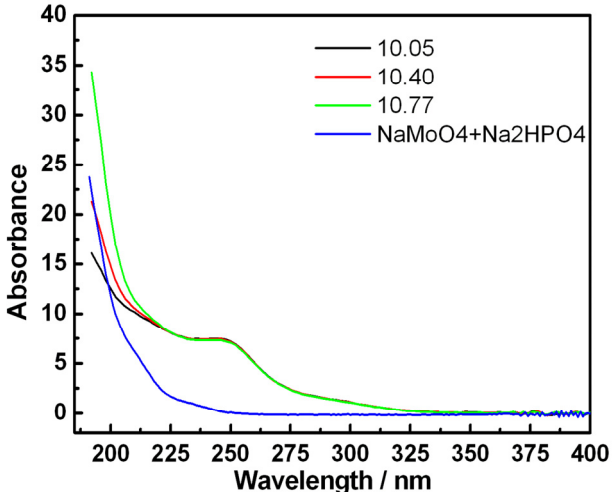

Fig. S12. Comparison between the UV spectra of **2** (pH > 9.70) and the UV spectrum of the mixture of $Na_2MoO_4{\cdot}2H_2O$ and Na_2HPO_4 with the molar ratio of 3:2 (pH = 10.50). The pH values were adjusted using diluted NaOH solution.

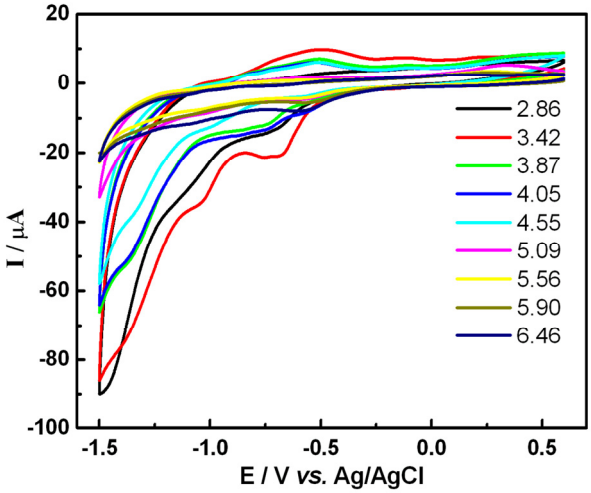

Fig. S13. Cyclic voltammograms of 1.0 mM **1** with the pH ≤ 6.46 region in 0.5 M Na_2SO_4 aqueous solution as the supporting electrolyte. Scan rate: 100 mV s^{-1}. The pH values of the acidic direction were adjusted using diluted H_2SO_4 solution. A three-electrode system was employed for cyclic voltammetry. A 4 mm diameter glassy carbon disk electrode (GCE) was used as a working electrode, a platinum wire served as the counter electrode and an Ag/AgCl electrode as the reference electrode.

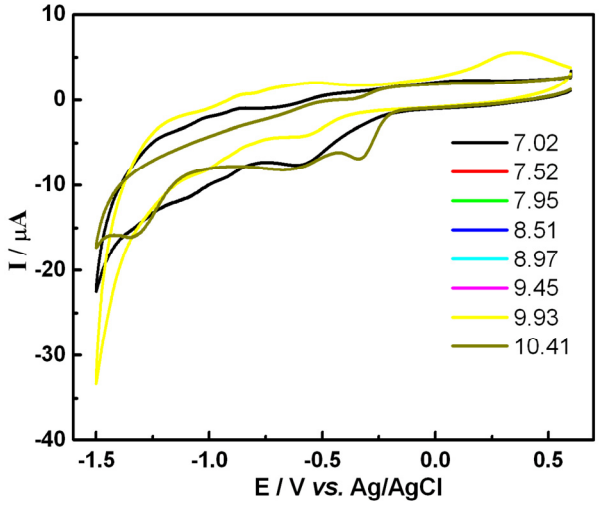

Fig. S14. Cyclic voltammograms of 1.0 mM **1** with the pH > 6.46 region in 0.5 M Na_2SO_4 aqueous solution as the supporting electrolyte. Scan rate: 100 mV s^{-1}. The pH values of the acidic direction were adjusted using diluted NaOH solution. The measurement conditions were as Fig. S13.

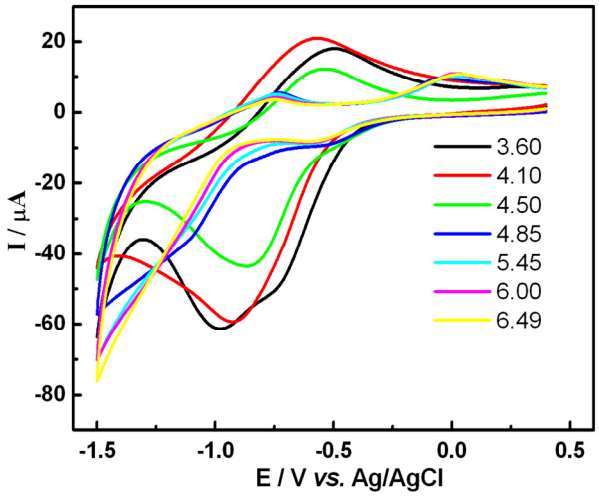

Fig. S15. Cyclic voltammograms of 1.0 mM **2** with the pH ≤ 6.49 region in 0.5 M Na_2SO_4 aqueous solution as the supporting electrolyte. Scan rate: 100 mV s^{-1}. The pH values of the acidic direction were adjusted using diluted H_2SO_4 solution. The measurement conditions were as Fig. S13.

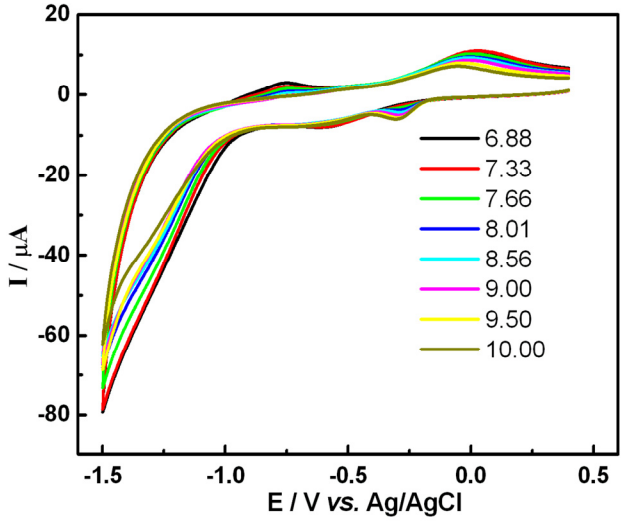

Fig. S16. Cyclic voltammograms of 1.0 mM **2** with the pH > 6.49 region in 0.5 M Na_2SO_4 aqueous solution as the supporting electrolyte. Scan rate: 100 mV s^{-1}. The pH values of the acidic direction were adjusted using diluted NaOH solution. The measurement conditions were as Fig. S13.

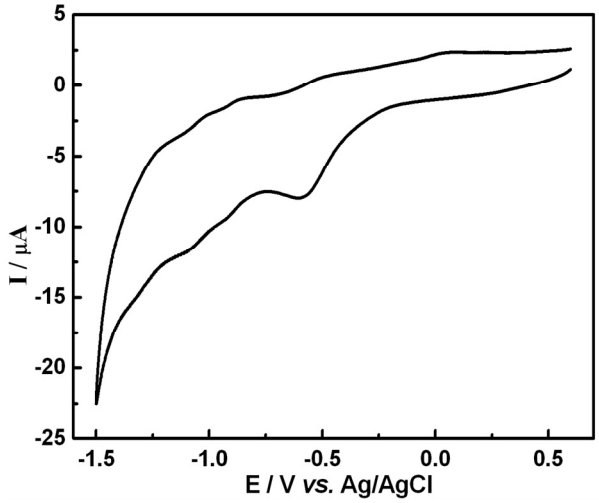

Fig. S17. Cyclic voltammogram of 1.0 mM **1** in 0.5 M Na_2SO_4 aqueous solution as the supporting electrolyte (At this point, the pH = 6.46). Scan rate: 100 mV s^{-1}.

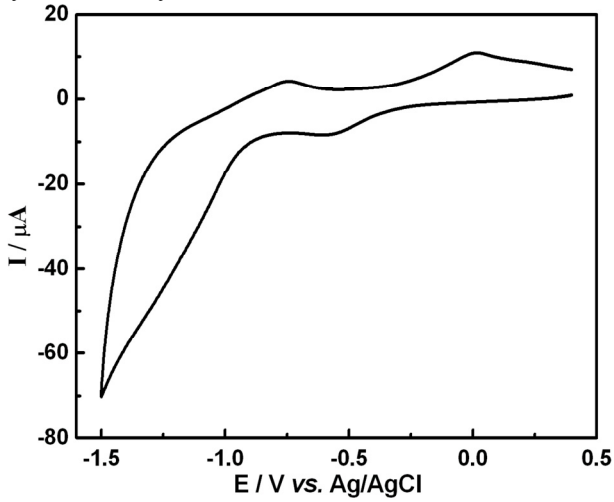

Fig. S18. Cyclic voltammogram of 1.0 mM **2** in 0.5 M Na_2SO_4 aqueous solution as the supporting electrolyte (At this point, the pH = 6.49). Scan rate: 100 mV s^{-1}.

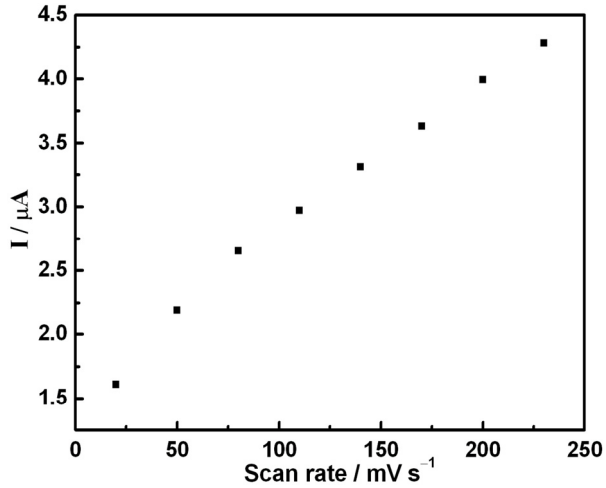

Fig. S19. Dependence of the peaks currents on the scan rates for 1.0 mM **1** in 0.5 M Na_2SO_4 aqueous solution (At this point, the pH = 6.46).

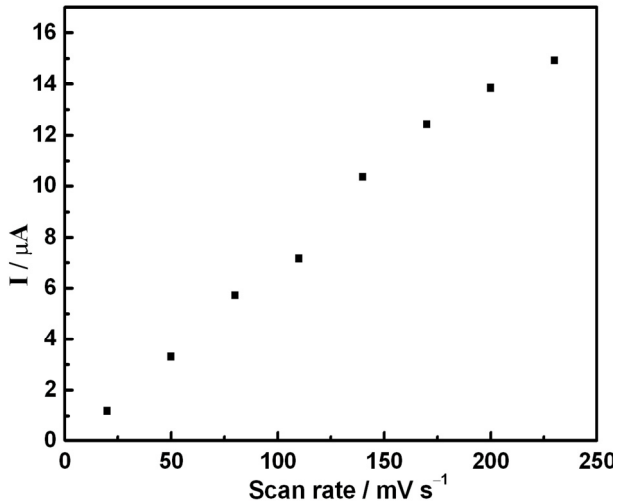

Fig. S20. Dependence of the peak currents on the scan rates for 1.0 mM **2** in 0.5 M Na_2SO_4 aqueous solution (At this point, the pH = 6.49).

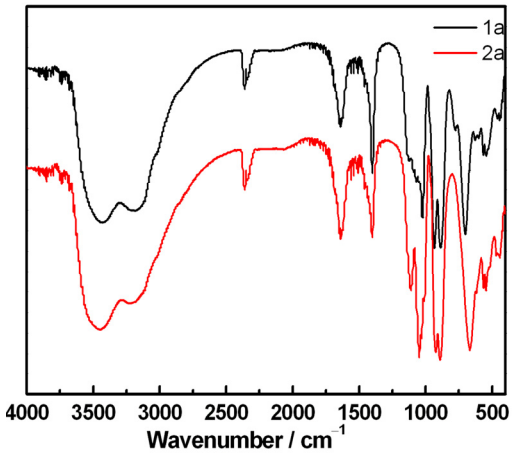

Fig. S21. IR spectra of **1a** and **2a**.